Vol 18 No 9, September 2009
1674-1056/2009/18(09)/3819-09

Chinese Physics B

© 2009 Chin. Phys. Soc.
and IOP Publishing Ltd

# Doubly excited 2s2p $^{1,3}P_1$ resonances in photoionization of helium*

Wan Jian-Jie(万建杰)[a] and Dong Chen-Zhong(董晨钟)[a)b)†]

[a] College of Physics and Electronic Engineering, Northwest Normal University, Lanzhou 730070, China
[b] Joint Laboratory of Atomic and Molecular Physics, NWNU & IMP CAS, Lanzhou 730070, China

(Received 15 November 2008; revised manuscript received 5 December 2008)

The multi-configuration Dirac–Fock (MCDF) method is implemented to study doubly excited 2s2p $^{1,3}P_1$ resonances of the helium atom and the interference between photoionization and photoexcitation autoionization processes. In order to reproduce the total photoionization sprectra, the excited energies from the ground $1s^2\ ^1S_0$ state to the doubly excited 2s2p $^{1,3}P_1$ states and the relevant Auger decay rates and widths are calculated in detail. Furthermore, the interference profile determined by the so-called Fano parameters $q$ and $\rho^2$ is also reproduced. Good agreement is found between the present results and other available theoretical and experimental results. This indeed shows a promising way to investigate the Fano resonances in photoionization of atoms within the MCDF scheme, although there are some discrepancies in the present calculations of the 2s2p $^3P_1$ state.

**Keywords:** MCDF method, doubly excited state, photoionization, Fano parameter, interference
**PACC:** 3120A, 3120T, 3280

## 1. Introduction

Since the Rydberg series of doubly excited states 2snp $^1P_1$ of the helium atom was discovered by Madden and Codling[1] through the photoabsorption experiment in the early 1960s, experimental and theoretical investigations on the doubly excited states have been carried out extensively. With the development of modern synchrotron radiation sources equipped with their associated high-resolution monochromators, more sophisticated and accurate photoionization experiments were performed, such as the investigation on Rydberg series above the first ionization threshold and higher ones of helium,[2−13] the decay properties of double excitations,[14−18] photoelectron angular distributions,[19] interseries interference,[20] dipole-quadrupole interference,[21,22] quantum chaos,[23] femtosecond induced transparency and absorption[24] and so on.

Besides the experiments, various theoretical methods have also been utilized to study the doubly excited states of helium in recent decades. For example, the interference effect of an isolated resonance on the total photoabsorption or total photoionization cross section was derived originally by Fano and coworkers.[25,26] At the same time, a new classification of the doubly excited states was set up by Cooper *et al*,[27] who stated that the classifications of the 2s$n$p and the 2p$n$s states did not constitute an appropriate zero-order approximation, because the states 2s$n$p and 2p$n$s are nearly degenerate; the electron–electron interaction, if sufficiently strong, will remove their degeneracy at the starting point of perturbation treatment and replace the symmetrized independent-electron wavefunctions $u\,(2sn\mathrm{p})$ and $u\,(2pn\mathrm{s})$ with the pair $\psi\,(2n\pm) = \{u\,(2sn\mathrm{p}) \pm u\,(2pn\mathrm{s})\}/\sqrt{2}$, only $\psi\,(22+) = u\,(2\mathrm{s}2\mathrm{p})$. Burke and McVicar[28] have treated the problem in the close-coupling approximation and have obtained values for the position, widths, and $q$ values of the low-lying resonances. Berrington *et al*[29] have carried out a six-state calculation by using the $R$-matrix program.[30] Bhatia and Temkin[31] have calculated the autoionizations of He and $H^-$ by using the Feshbach projection-operator formalism. Lipsky and Conneely[32] have used a procedure combining the truncated diagonalization method (TDM) with

*Project supported by the National Natural Science Foundation of China (Grant Nos 10774122 and 10876028), the China/Ireland Science and Technology Collaboration Research Fund (Contract No CI-2004-07), the Specialized Research Fund for the Doctoral Program of Higher Education of China (Grant No 20070736001) and the Foundation of Northwest Normal University of China (Grant No NWNU-KJCXGC-03-21).
†E-mail: dongcz@nwnu.edu.cn

the open-channel close coupling approximation to calculate widths of autoionization states in two-electron systems. McGreevy and Stewart[33] have determined the position and width of the 2s2p $^1P_1$ autoionization state of helium by using perturbation theory. Complex-coordinate calculations for doubly excited states have also been carried out for the double excitations of helium by Domke *et al*,[12] Ho,[34,35] Chung and Davis[36] and Bentley.[37] Salomonson *et al*[38] have implemented a multichannel coupled-equation calculation in the framework of many-body perturbation (MBPT) theory. A $K$-matrix method employing $L^2$ basis sets has also been utilized to investigate the $^1P_1$ continuum of helium in an energy region from 65.4 to 73.0 eV by Moccia and Spizzo.[39] The hyperspherical close-coupling method combined with the multichannel quantum-defect theory (MQDT) was employed to study the very narrow doubly excited $^1P_1$ state of helium by Tang *et al.*[40] Based on the relativistic multichannel theory (RMCT), the positions and the widths of doubly excited $^1P_1$ resonances have been calculated by Zou *et al.*[41] Gorczyca *et al*[42] have investigated the near-threshold photofluorescence behaviour by carrying out a detailed numerical calculation within an $R$-matrix multichannel quantum defect theory (MQDT). Hence two-electron dynamics remains an active field of research up to the present day.

However, there are still a few studies on doubly excited states by the multi-configuration Dirac–Fock (MCDF) method[43,44] that were hardly used to study the (interference) Fano resonances in photoionization spectra. From the theoretical point of view, it is interesting to return to the study of doubly excited states with the aid of the fully relativistic MCDF method. Undoubtedly, the MCDF theory can also be used to investigate the interference properties of doubly excited states, so the lightest helium atom, of course, becomes the first sample in our theoretical work.

## 2. Theoretical method

To start with, the eigenvalues of the ground state 1s$^2$ $^1S_0$ and doubly excited states 2s2p $^{1,3}P_1$, the energy differences and the corresponding bound-bound and continuum-bound transition matrix elements are calculated by using two new components REOS99[45] and AUGER[46] of RATIP package[47] and a newly developed relativistic photoionization program RERR06[48,49] based on the MCDF method. Then, the interference between photoionization and photoexcitation autoionization, i.e.

$$\hbar\omega + 1\mathrm{s}^2\ {}^1S_0 \rightarrow 1\mathrm{s} + \mathrm{e}^- \tag{1}$$

and

$$\hbar\omega + 1\mathrm{s}^2\ {}^1S_0 \rightarrow 2\mathrm{s}2\mathrm{p}\ {}^{1,3}P_1 \rightarrow 1\mathrm{s} + \mathrm{e}^- \tag{2}$$

is also studied in detail.

The interference effect of an isolated resonance on the total photoionizaton cross section was derived originally by Fano and coworkers.[25,26] The expression for the total cross section $\sigma(\omega)$ for a photon of energy $\omega$ in the case of a single discrete state interacting with one or more continuum states is as follows:

$$\sigma(\omega) = \sigma_{\mathrm{if}}^{\mathrm{PI}}(\omega)\left(\rho_{\mathrm{ijf}}^2\frac{(q_{\mathrm{ijf}}+\tilde{\omega})^2}{1+\tilde{\omega}^2} + 1 - \rho_{\mathrm{ijf}}^2\right), \tag{3}$$

where $\sigma_{\mathrm{if}}^{\mathrm{PI}}(\omega)$ is the direct photoionization cross section from initial ionic state i to final ionic state f, and

$$\tilde{\omega} = \frac{\omega - E_{\mathrm{r}}}{\frac{1}{2}\Gamma} = \frac{\omega - E_{\mathrm{ji}} - \Delta_{\mathrm{r}}}{\frac{1}{2}\Gamma} \tag{4}$$

describes the departure of the incident photon energy $\omega$ from a resonance centre $E_{\mathrm{r}} = E_{\mathrm{ji}} + \Delta_{\mathrm{r}}$, where $E_{\mathrm{ji}} \equiv E_{\mathrm{j}} - E_{\mathrm{i}}$ is the resonance energy between initial state i and resonant state j and the quantity $\Delta_{\mathrm{r}}$ represents thus a shift of the resonance centre with respect to $E_{\mathrm{ji}}$. The shift is regarded as approximately zero in practical calculations so that the resonance centre is given only by $E_{\mathrm{ji}}$. $\Gamma$ is the linewidth of the resonance, which is considered as a sum of Auger and radiative widths. However, in the case of 2s2p $^{1,3}P_1$, their radiative widths are rather less than their Auger ones, so the linewidth is assumed to be the Auger width given by

$$\Gamma^{\mathrm{auger}} = 2\pi\sum_{\kappa}\left|\langle\Psi_{\mathrm{f}}, \varepsilon\kappa;\ \Psi_{\mathrm{f}'}\left\|\sum_{p<q}V_{pq}\right\|\Psi_{\mathrm{j}}\rangle\right|^2, \tag{5}$$

where $\Psi_{\mathrm{j}}$ is the atomic state function (ASF) of the autoionization state j, while $\Psi_{\mathrm{f}'}$ is the ASF of the system formed by an ionic state $\Psi_{\mathrm{f}}$ and a continuum electron $\kappa$ with energy $\varepsilon$. The two-electron operator $V_{\mathrm{pq}}$ in expression (5) is the sum of Coulomb and Breit operators, which has the form in atomic units

$$V_{pq} = \frac{1}{r_{pq}} - \boldsymbol{\alpha}_p\cdot\boldsymbol{\alpha}_q\frac{\cos(\omega_{pq}r_{pq})}{r_{pq}} + (\boldsymbol{\alpha}_p\cdot\nabla_p)(\boldsymbol{\alpha}_q\cdot\nabla_q)\frac{\cos(\omega_{pq}r_{pq})-1}{\omega_{pq}^2 r_{pq}}, \tag{6}$$

where $\boldsymbol{\alpha}_p$ and $\boldsymbol{\alpha}_q$ are the Dirac vector matrixes, and $\omega_{pq}$ is the wave number of the exchanged virtual photon, and the Auger rate $A_{\mathrm{jf}}^{\mathrm{a}}$ is equal to the Auger linewidth in atomic units.

The nonresonance background cross section is given by[48,49]

$$\sigma_{\mathrm{if}}^{\mathrm{PI}}(\omega) = 2\pi^2 a_0^2 \alpha \frac{\mathrm{d}f_{\mathrm{if}}}{\mathrm{d}\varepsilon}, \tag{7}$$

where $a_0$ is the Bohr radius, $\alpha$ is the fine structure constant and $\omega$ indicates the incident photon energy which yields, according to the energy conservation law,

$$\varepsilon = E_{\mathrm{if}} + \omega, \tag{8}$$

$$E_{\mathrm{if}} \equiv E_{\mathrm{i}} - E_{\mathrm{f}}, \tag{9}$$

and the so-called oscillator strength density is given as follows:[48,49]

$$\frac{\mathrm{d}f_{\mathrm{if}}}{\mathrm{d}\varepsilon} = \frac{\pi c}{(2L+1)\,\omega^2} \sum_{\kappa,L} \left| \left\langle \Psi_{\mathrm{f}}, \varepsilon\kappa;\, \Psi_{\mathrm{f}'} \left\| O^{(\mathrm{L})} \right\| \Psi_{\mathrm{i}} \right\rangle \right|^2, \tag{10}$$

where $\Psi_{\mathrm{i}}$ is the ASF of the initial state i, while $\Psi_{\mathrm{f}'}$ is the ASF of the system formed by an ionic state $\Psi_{\mathrm{f}}$ and a continuum electron $\kappa$ with energy $\varepsilon$, $\omega$ is the energy of the incident photon, $c$ is the speed of light.

The Fano parameters $q$ and $\rho^2$ can be expressed in terms of the radiative transition matrix elements for transitions from the initial state $|\Psi_{\mathrm{i}}\rangle$ to the discrete state $|\Psi_{\mathrm{j}}\rangle$, and to the continuum state $|\Psi_{\mathrm{f}}, \varepsilon\kappa;\, \Psi_{\mathrm{f}'}\rangle$, together with the Coulomb interaction matrix elements coupling the discrete state to the continuum. The Fano parameter $q$, which governs the (interference) shape of the total cross section, is given by

$$q_{\mathrm{ijf}} = \frac{\left\langle \Phi_{\mathrm{j}} \left\| O^{(\mathrm{L})} \right\| \Psi_{\mathrm{i}} \right\rangle}{\pi \sum_{\kappa} \left\langle \Psi_{\mathrm{j}} \left\| \sum_{p<q} V_{pq} \right\| \Psi_{\mathrm{f}}, \varepsilon\kappa;\, \Psi_{\mathrm{f}'} \right\rangle \left\langle \Psi_{\mathrm{f}}, \varepsilon\kappa;\, \Psi_{\mathrm{f}'} \left\| O^{(\mathrm{L})} \right\| \Psi_{\mathrm{i}} \right\rangle}, \tag{11}$$

and the correlation coefficient $\rho^2$, which is a measure of the strength of the resonance, is defined as

$$\rho_{\mathrm{ijf}}^2 = \frac{\left[ \sum_{\kappa} \left\langle \Psi_{\mathrm{j}} \left\| \sum_{p<q} V_{pq} \right\| \Psi_{\mathrm{f}}, \varepsilon\kappa;\, \Psi_{\mathrm{f}'} \right\rangle \left\langle \Psi_{\mathrm{f}}, \varepsilon\kappa;\, \Psi_{\mathrm{f}'} \left\| O^{(\mathrm{L})} \right\| \Psi_{\mathrm{i}} \right\rangle \right]^2}{\left[ \sum_{\kappa} \left( \left\langle \Psi_{\mathrm{j}} \left\| \sum_{p<q} V_{pq} \right\| \Psi_{\mathrm{f}}, \varepsilon\kappa;\, \Psi_{\mathrm{f}'} \right\rangle \right)^2 \right] \left[ \sum_{\kappa} \left( \left\langle \Psi_{\mathrm{f}}, \varepsilon\kappa;\, \Psi_{\mathrm{f}'} \left\| O^{(\mathrm{L})} \right\| \Psi_{\mathrm{i}} \right\rangle \right)^2 \right]}, \tag{12}$$

where $O^{(\mathrm{L})}$ represents the radiative operator and $\Phi_{\mathrm{j}}$ is the discrete state modified by an admixture of the continuum states. The degree to which $\Phi_{\mathrm{j}}$ is different from $\Psi_{\mathrm{j}}$ is dependent upon the energy variations of the continuum wavefunctions in the proximity of the resonance. In the present work, it is easy to replace $\Phi_{\mathrm{j}}$ with $\Psi_{\mathrm{j}}$ approximately. While the matrix elements in expressions (11) and (12) are not strictly energy independent, they are slowly varying functions of energy, and the values of $\sigma_{\mathrm{if}}^{\mathrm{PI}}(\omega)$, $\Gamma$, $q$ and $\rho^2$ are assumed to be constant in the vicinity of the resonance.

## 3. Results and discussion

To investigate the (interference) Fano profle at the doubly excited states 2s2p $^{1,3}P_1$ in the photoionization of helium $1s^2\ ^1S_0$, it is necessary to investigate all the ionic level structures and excitation/ionization energies, Auger decay properties of the resonance states, direct photoionization cross sections as well as the corresponding transition matrix elements.

As is known, when an electron is ionized or a photon is emitted from an atom or ion, the charge density of residual electrons will rearrange due to the changed potential and this is called orbital relaxation. As far as we know, orbital relaxation is a normal phenomenon in various dynamical processes, especially for neutral atoms and lowly charged ions. As the simplest multi-electron atom, helium's electronic 'orbitals' can redistribute during transition processes such as excitation, ionization, radiative and Auger transition and so on. To demonstrate the effects, a separate generation of

the wavefunctions for the initial and final states of a given transition has been carried out. Table 1 gives the mean radii of occupied 1s, 2s, $2p_{1/2}$ and $2p_{3/2}$ orbitals, where 1s orbitals in $1s^2\ ^1S_0$ and $1s\ ^2S_{1/2}$ states are denoted as 1s and 1s′ respectively for convenience.

As seen from Table 1, the mean radius of 1s, whether it is in $1s^2$ or 1s, is much smaller than those of 2s, $2p_{1/2}$ and $2p_{3/2}$ in $2s2p\ ^{1,3}P_1$ states. The size of the atom has definitely contracted considerably both for the one-photon-two-electron transition from $1s^2\ ^1S_0$ to $2s2p\ ^{1,3}P_1$ and the Auger decay from $2s2p\ ^{1,3}P_1$ to $1s\ ^2S_{1/2}$, but the orbital contraction for the photoionization from $1s^2\ ^1S_0$ to $1s\ ^2S_{1/2}$ is relatively small. Its direct effect is to make the orbital overlap between the initial and the final states nonorthognormal. They are $\langle 1s'|1s\rangle = 0.984$, $\langle 2s|1s\rangle = -0.121$, and $\langle 1s'|2s\rangle = 0.00796$. So the relaxation effects in radiative transitions should be considered in this work.

**Table 1.** Mean radii of occupied orbitals in the ground and doubly excited states (in atomic units).

| states | orbitals | $< r >$ |
|---|---|---|
| $1s^2\ ^1S_0$ | 1s | 0.927 |
| $1s\ ^2S_{1/2}$ | 1s′ | 0.750 |
| | 2s | 3.720 |
| $2s2p\ ^{1,3}P_1$ | $2p_{1/2}$ | 2.912 |
| | $2p_{3/2}$ | 2.878 |

As far as neutral atoms and lowly charged low-$Z$ ions are concerned, in addition to the electron relaxation, electron correlation also plays a very important role in atomic structures. Here, as shown above, an independent calculation of obitals for the $1s^2\ ^1S_0$ ground state and for the $J^{\rm P} = 1^-$ level group of the 2s2p configuration has been carried out where the electron relaxation is taken into account. On the other hand, the electron correlation can be considered by enlarging the expansion of the ASF with the same symmetry in the framework of MCDF method. In order to include a sufficiently large number of configuration state functions (CSFs) in the expansion of the ASF, the active space method as discussed by Roos *et al*[50] is used to generate the configuration state list systematically.[51] Then the relaxed MCDF calculation in the extensive optimized level (EOL) scheme is implemented in the present work.

To investigate the effects of the size of the wavefunctions on excitation/ionization energies and transition properties, a series of large-scale MCDF computations is carried out for the selected levels and transitions between those levels by using different correlation models. Apart from the single configuration (SC) model originating from Cooper *et al*'s zeroth classification,[27] all virtual single (S) and double (D) excitations from the occupied shells, i. e. 1s in the ground state and 2s and 2p in the doubly excited states, into the unoccupied subshells are taken into account. For the ground state, the unoccupied subshells include {2s, 2p}, {3s, 3p, 3d}, {4s, 4p, 4d, 4f}, {5s, 5p, 5d, 5f, 5g} and {6s, 6p, 6d, 6f, 6g, 6h}. For the doubly excited states, the virtual orbitals include {1s}, {3s, 3p, 3d}, {4s, 4p, 4d, 4f}, {5s, 5p, 5d, 5f, 5g} and {6s, 6p, 6d, 6f, 6g, 6h}. For the sake of brevity, these models are denoted by 2SD, 3SD, 4SD, 5SD and 6SD, respectively. For example, 3SD model represents the excitation to {2s, 2p} and {3s, 3p, 3d} for the ground state and for the excitation to {1s} and {3s, 3p, 3d} for the doubly excited states.

Table 2 shows the number of CSFs which are utilized in the wave function expansion of the corresponding $J^{\rm P}$ level groups with a given total angular momentum and parity. For the representation of the $2s2p\ ^{1,3}P_1$ levels, for instance, the 6SD correlation model results in 180 CSFs as used for the diagonalization of the Dirac–Coulomb–Breit Hamiltonian matrix.

In the present calculations, the (transverse) Breit interactions are also added by diagonalizing the Dirac–Coulomb–Breit Hamiltonian matrix. The nucleus finite size and motion effects are also considered. In addition, the dominant quantum electrodynamic (QED) contributions, i.e. self-energy and vacuum polarization effects, are also included in the computations of energies in the hydrogen-like approximation and as perturbation, although QED effects are very slight for light atoms.

**Table 2.** Some possible correlation models and numbers of CSFs, in the ASF expansion for several selected level groups.

| model | $1s^2\ \ ^1S_0$ | $2s2p\ ^{1,3}P_1$ |
|---|---|---|
| SC | 1 | 2 |
| 2SD | 5 | 4 |
| 3SD | 14 | 18 |
| 4SD | 30 | 48 |
| 5SD | 55 | 100 |
| 6SD | 91 | 180 |

Table 3 gives the ionization and excitation energies as the size of the wave function expansions increases systematically. In all these cases, the SC approximation provides only a rough estimate of the ion-

ization and the excitation energies which cannot be used for analysis in highly accurate experiments. Instead, the SD excitations into the high-$n$l subshells are required to obtain theoretical energies in reasonable agreement with experimental results. It can be seen that the present eigenvalues and energy differences are in good agreement with the experimental results[1,2,5,8,9,12,13] as well as other accurate theoretical calculations.[28,29,31,32,34,35,37−40,42,52−55] It is noted that the relative error of the present energy for the ground state is less than 0.01% compared with the experimental value −79.0052 eV[9] and that both the nonrelativistic variational[52,53] and MCDF calculations together with an extrapolation[54] are lower than the experimental value, as Duan *et al*[55] pointed out, because the motion of the nucleus has not been considered in Refs.[52]–[54].

For the doubly excited 2s2p $^{1,3}P_1$ states, it is clear that the results presented in Table 3 are also convergent with the number of CSFs increasing. From the comparison of our results with other available experimental and theoretical values, it should be suggested that excitations into higher subshells become necessary if the theoretical excitation energies are expected to be accurate to better than 0.1%. Even so, it is noted that the results for the $^3P_1$ level are in agreement with other theoretical results for the $^3P$ term[31,32,34,35,37,39] due to the small splitting between the individual levels of the term. So more detailed MCDF calculations on the triplet 2s2p $^3P_{0,1,2}$ states are desired in the future.

Table 4 displays the influences of various correlation models on the Auger decay rates and widths of 2s2p $^{1,3}P_1$. As seen from the table, the rates and the widths are much closer to each other from the 5SD to the 6SD models. From the comparison of the two states, moreover, we see that a rather different trend and convergence take place with the number of CSFs increasing. The theoretical results for triplet state vary considerably from the SC to the 6SD models, which shows more influence of configuration interaction on its Auger rate and width than that of the singlet state. This trend is similar to that for the calculations that Bentley[37] obtained by the complex-coordinate Hartree–Fock method. Additionally, as Moccia and Spizzo pointed out,[39] the width of the 2s2p $^3P$ resonance may be a controversial question. In 1983, Cederquist *et al*[4] analysed the decays from the levels 2p3p $^3P$, 2p3p $^3D$ and 2p4p $^3D$ to the 2s2p $^3P$ resonance and obtained linewidths of 7.12 ± 0.12, 8.36 ± 0.08 and 8.32 ± 0.15 meV respectively. In their work, the radiative widths were negligible and the first result was considered as the best. In spite of the discrepancy between our results and the experimental results, we believe that the present width of 2s2p $^3P_1$ is reasonable because the experimental value should be the total width of 2s2p $^3P_{0,1,2}$. Maybe a good many further correlations are needed in order to obtain a more accurate description of them; to some extent we still accept the agreement between the present results and other theoretical[28,29,31−41] and experimental[2,4,5,8,12,13,21] ones.

Based on the convergent energies and Auger rates and widths to an acceptable extent, the photoabsorption oscillator strength is convergent to $5.46.\times10^{-7}$ (Babushkin) and $6.72.\times10^{-7}$ (Coulomb) for the 2s2p $^3P_1$ resonance, $4.33.\times10^{-3}$ (Babushkin) and $3.34.\times10^{-3}$ (Coulomb) for the 2s2p $^1P_1$ resonance in the 6SD model. Meanwhile, the photoionization cross sections at the 2s2p $^{1,3}P_1$ resonances have been calculated and they are 1.13 and 1.22 Mb in the Babushkin gauge, 1.25 and 1.35 Mb in the Coulomb gauge, respectively. Finally, the Fano parameters $q$ and $\rho^2$ in both the Babushkin and Coulomb gauges have also been calculated for two 2s2p $^{1,3}P_1$ levels as shown in Table 5, by using the relevant transition matrix elements to determine these convergent results.

Additionally, it is interesting to mention that in the nonrelativistic treatment this is a single-continuum problem and the $\rho^2$ parameter is a constant (unity), but in the relativistic framework it becomes a double-continuum problem. With the comparison, our results are in reasonable agreement with the results obtained from experiments[2,5,8,12,13,21] and other nonrelativistic theoretical methods.[28,29,31,38,39] The interference spectra are also shown in Fig.1, where the relativistic $R$-matrix spectra[55] are plotted too. From the figure, the interference spectra with the present parameters in the Babushkin gauge are in better accordance with those from the DARC[55] and the experiment,[9] although there may be something unexplained in the present results for the 2s2p $^3P_1$ state.

**Table 3.** The values of total binding energy $E$ and the energy difference $\Delta E$ relative to the ground state $1s^2\ ^1S_0$ (eV).

| model | $1s^2\ ^1S_0$ | | $1s\ ^2S_{1/2}$ | | $2s2p\ ^3P_1$ | | | $2s2p\ ^1P_1$ | | | |
|---|---|---|---|---|---|---|---|---|---|---|---|
| | $E$ | $\Delta E$ | $E$ | $\Delta E$ | $E$ | $\Delta E$ | | $E$ | $\Delta E$ | | |
| SC | –77.862 | 0 | –54.418 | 23.443 | –20.439 | 57.422 | | –17.772 | 60.090 | | |
| 2SD | –78.840 | 0 | –54.418 | 24.422 | –20.424 | 58.416 | | –17.774 | 61.066 | | |
| 3SD | –78.953 | 0 | –54.418 | 24.535 | –20.664 | 58.289 | | –18.781 | 60.172 | | |
| 4SD | –78.982 | 0 | –54.418 | 24.564 | –20.668 | 58.314 | | –18.786 | 60.196 | | |
| 5SD | –78.993 | 0 | –54.418 | 24.575 | –20.675 | 58.318 | | –18.804 | 60.190 | | |
| 6SD | –78.998 | 0 | –54.418 | 24.580 | –20.676 | 58.322 | | –18.811 | 60.188 | | |
| other theory | | | | | | | | | | | |
| | –79.014[52] | | | 24.588[42] | –20.633[32] | 58.321[31] | 58.308[37IV] | –18.730[32] | 60.269[28] | 61.091[37I] | 60.154[39I] |
| | –79.014[53] | | | | –20.694[34,35] | 58.375[32] | 58.305[37V] | –18.861[34] | 60.169[29] | 60.290[37II] | 60.155[39II] |
| | –79.018[54] | | | | | 58.321[34] | 58.310[39I] | | 60.145[31] | 60.214[37III] | 60.154[39III] |
| | –79.005[56] | | | | | 58.499[37I] | 58.310[39II] | | 60.277[32] | 60.197[37V] | 60.188[40] |
| | | | | | | 58.364[37II] | 58.309[39III] | | 60.146[34] | 60.266[38I] | |
| | | | | | | 58.309[37III] | | | 60.149[36] | 60.184[38II] | |
| experiment | | | | | | | | | | | |
| | –79.005[9] | | | | | | | | 60.1[1] | 60.151(10)[5] | 60.147(1)[12] |
| | | | | | | | | | 60.123(15)[2] | 60.133(15)[8] | 60.150(4)[13] |

Note: The numbers in the parentheses are the uncertainties in the corresponding experimental values throughout the paper. For $2s2p\ ^3P_1$, the available theoretical values are given only for the $2s2p\ ^3P$ term. In Ref.[37], *I*–*V* represent two-, three-, four-, five-, and six-configuration calculations, respectively. In Ref.[38], I and II denote four- and nine-channel results, respectively. In Ref.[39], I–III refer to the results given by phase-shift analysis, complex stabilization and the Fano method, respectively.

**Table 4.** Contribution of correlation effects to Auger decay rates.

| | Auger rate/$s^{-1}$ | | Auger width/meV | | | | |
|---|---|---|---|---|---|---|---|
| | 2s2p $^3P_1$ | 2s2p $^1P_1$ | 2s2p $^3P_1$ | | 2s2p $^1P_1$ | | |
| SC | 1.54[13] | 9.38[13] | 10.12 | | 61.74 | | |
| 2SD | 8.69[12] | 7.91[13] | 5.72 | | 52.05 | | |
| 3SD | 3.46[12] | 6.10[13] | 2.28 | | 40.14 | | |
| 4SD | 3.22[12] | 5.99[13] | 2.12 | | 39.43 | | |
| 5SD | 2.98[12] | 5.83[13] | 1.96 | | 38.36 | | |
| 6SD | 3.05[12] | 5.84[13] | 2.01 | | 38.42 | | |
| other theory | | | | | | | |
| | | | 8.90[31] | 0.40[37III] | 43.8[28] | 37.36[36] | 37.0[39I] |
| | | | 13.92[32] | 0.34[37IV] | 38.6[29] | 42.19[37I] | 34.6[39II] |
| | | | 8.08[34] | 0.33[37V] | 36.3[31] | 43.20[37II] | 36.5[39III] |
| | | | 8.13[35] | 8.18[39] | 34.05[32] | 30.03[37III] | 46.9[40] |
| | | | 9.88[37I] | 8.25[39] | 36.5[33I] | 30.10[37V] | 37.3[41] |
| | | | 9.68[37II] | 8.01[39] | 37.4[33II] | 43.7[38I] | |
| | | | | | 37.14[34] | 40.3[38II] | |
| experiment | | | | | | | |
| | | 5.8(6)[13][2] | 7.12(12)[4] | | 38(4)[2] | 38(1)[8] | 37.6(2)[13] |
| | | | | | 38(2)[5] | 37(1)[12] | 37.9(10)[21] |

Note: The numbers in the square brackets refer to the power of ten. For 2s2p $^3P_1$, the available experimental and theoretical values are given only for the 2s2p $^3P$ term.

**Table 5.** Comparison of the calculated Fano parameters $q$ and $\rho^2$ with previous computations and measurements for two 2s2p $^{1,3}P_1$ levels which are denoted as the LS coupling scheme.

| state | method | $q$ | | $\rho^2$ | |
|---|---|---|---|---|---|
| | | $B$ | $C$ | $B$ | $C$ |
| $^3P_1$ | this work | 1.10 | 1.58 | 0.01 | 0.01 |
| $^1P_1$ | this work | –2.64 | –2.20 | 0.99 | 0.99 |
| | other theory | | | | |
| | Ref.[28] | –2.59 | –2.65 | | |
| | Ref.[29] | –2.83 | –2.95 | | |
| | Ref.[38I] | –2.56 | –2.66 | | |
| | Ref.[38II] | –2.63 | –2.70 | | |
| | Ref.[39] | –2.78 | –2.77 | | |
| | Ref.[31] | –2.29 | | | |
| | experiment | | | | |
| | Ref.[2] | –2.80(25) | | | |
| | Ref.[5] | –2.6(3) | | | |
| | Ref.[8] | –2.75(5) | | | |
| | Ref.[12] | –2.75(1) | | | |
| | Ref.[13] | –2.73(4) | | | |
| | Ref.[21] | –2.74(5) | | | |

Note: $B$ and $C$ refer to the Babushkin and Coulomb gauges, which become the length ($L$) and velosity ($V$) gauges in the nonrelativistic limit, respectively.

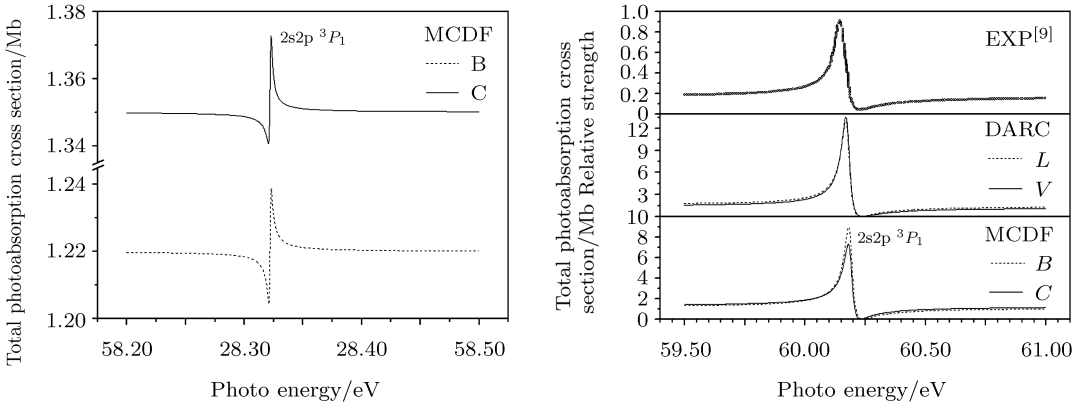



**Fig.1.** Comparison between the total photoabsorption cross sections from 58.2 to 61.0 eV with the experimental spectra from Ref.[9], where the relativistic $R$-matrix calculation is obtained by using DARC code[57] for doubly excited 2s2p $^{1,3}P_1$ resonances.

# 4. Conclusion

We have shown the general procedure for investigating the (interference) Fano resonances within the framework of the MCDF method. Firstly, we systematically study the influence of correlation effects including the effects of relaxation on the level energies of the ground $1s^2$ state and the doubly excited 2s2p $^{1,3}P_1$ states of atomic helium as well as on their Auger transition rates and widths by using large-scale MCDF wavefunctions. As found from this study, relaxation and correlation effects play a key role in the wavefunctions, the total binding energies, excited energies, Auger rates and widths, and other transition properties. Secondly, the interference Fano parameters $q$ and $\rho^2$ can be obtained by using the transition matrix elements which lead to convergent calculations. In addition, the calculations for 2s2p $^3P_1$ puzzle us, but it is satisfactory to obtain convergent results in the present correlation models. Compared with previous computations and measurements, the present results provide not only consistent data for the low-lying doubly excited levels but also show a promising way to study doubly excited states in the framework of the MCDF method. In particular, the relativistic MCDF method is hopeful for studying the interference of doubly excited resonances of highly charged He-like ion in a more natural way. The present work aims mainly to demonstrate that the MCDF methods can yield results of high accuracy, comparable with the most accurate theoretical results available to date. Of course, we also know that there are some difficulties in working out the problem of overlapping resonances, especially with multi-continuum, by directly using the MCDF method, but it can play an important role in interpreting some detailed interference structures for relatively simple cases such as single or double-continuum processes and can easily be combined with the $R$-matrix method to study more complicated processes, thereby overcoming its weakness.

# Acknowledgement

One of the authors (Wan Jian-Jie) thanks Dr. Wang Guo-Li of Northwest Normal University in China for his relativistic $R$-matrix calculations and Professor Kanti M. Aggarwal of Queen's University of Belfast for valuable discussions.

# References

[1] Madden R P and Codling K 1963 *Phys. Rev. Lett.* **10** 516

[2] Madden R P and Codling K 1965 *Astrophys. J.* **141** 364

[3] Woodruff P R and Samson J A R 1982 *Phys. Rev.* A **25** 848

[4] Cederquist H, Kisielinski M and Mannervik S 1983 *J. Phys.* B **16** L479

[5] Morgan H D and Ederer D L 1984 *Phys. Rev.* A **29** 1901

[6] Lindle D W, Ferrett T A, Becker U, Kobrin P H, Truesdale C M, Kerkhoff H G and Shirley D A 1985 *Phys. Rev.* A **31** 714

[7] Lindle D W, Ferrett T A, Heimann P A and Shirley D A 1987 *Phys. Rev.* A **36** 2112
[8] Kossmann H, Krässig B and Schmidt V 1988 *J. Phys.* B **21** 1489
[9] Domke M, Xue C, Puschmann A, Mandel T, Hudson E, Shirley D A, Kaindl G, Greene C H, Sadeghpour H R and Petersen H 1991 *Phys. Rev. Lett.* **66** 1306
[10] Domke M, Remmers G and Kaindl G 1992 *Phys. Rev. Lett.* **69** 1171
[11] Domke M, Schulz K, Remmers G, Gutiérrez A, Kaindl G and Wintgen D 1995 *Phys. Rev.* A **51** R4309
[12] Domke M, Schulz K, Remmers G, Kaindl G and Wintgen D 1996 *Phys. Rev.* A **53** 1424
[13] Schulz K, Kaindl G, Domke M, Bozek J D, Heimann P A, Schlachter A S and Rost J M 1996 *Phys. Rev. Lett.* **77** 3086
[14] Menzel A, Frigo S P, Whitfield S B, Caldwell C D, Krause M O, Tang J Z and Shimamura I 1995 *Phys. Rev. Lett.* **75** 1479
[15] Rubensson J E, Såthe C, Cramm S, Kessler B, Stranges S, Richter R, Alagia M and Coreno M 1999 *Phys. Rev. Lett.* **83** 947
[16] Odling-Smee M K, Sokell E, Hammond P and MacDonald M A 2000 *Phys. Rev. Lett.* **84** 2598
[17] Coreno M, Prince K C, Richter R, de Simone M, Bučr K and Žitnik M 2005 *Phys. Rev.* A **72** 052512
[18] Söderström J, Agåker M, Zimina A, Feifel R, Eisebitt S, Follath R, Reichardt G, Schwarzkopf O, Eberhardt W, Mihelič A, Žitnik M and Rubensson J E 2008 *Phys. Rev.* A **77** 012513
[19] Menzel A, Frigo S P, Whitfield S B, Caldwell C D and Krause M O 1996 *Phys. Rev.* A **54** 2080
[20] Püttner R, Domke M, Grémaud B, Martins M, Schlachter A S and Kaindl G 1999 *J. Electron Spectrosc. Relat. Phenom.* **101–103** 27
[21] Krässig B, Kanter E P, Southworth S H, Guillemin R, Hemmers O, Lindle D W, Wehlitz R and Martin N L S 2002 *Phys. Rev. Lett.* **88** 203002
[22] Kanter E P, Krässig B, Southworth S H, Guillemin R, Hemmers O, Lindle D W, Wehlitz R, Amusia M Ya, Chernysheva L V and Martin N L S 2003 *Phys. Rev.* A **68** 012714
[23] Schlachter A S 2006 *Radiation Physics and Chemistry* **75** 2159
[24] Loh Z H, Greene C H and Leone S R 2008 *Chemical Physics* **350** 7
[25] Fano U 1961 *Phys. Rev.* **124** 1866
[26] Fano U and Cooper J W 1965 *Phys. Rev.* **137** A 1364
[27] Cooper J W, Fano U and Prats F 1963 *Phys. Rev. Lett.* **10** 518
[28] Burke P G and McVicar D D 1965 *Proc. Phys. Soc.* **86** 989
[29] Berrington K A, Burke P G, Fon W C and Taylor K T 1980 *J. Phys.* B **15** L603
[30] Berrington K A, Burke P G, Le Dourneuf M, Robb W D, Taylor K T and Vo Ky Lan 1978 *Comput. Phys. Commum.* **14** 367
[31] Bhatia A K and Temkin A 1975 *Phys. Rev.* A **11** 2018
[32] Lipsky L and Conneely M J 1976 *Phys. Rev.* A **14** 2193
[33] McGreevy E and Stewart A L 1977 *J. Phys.* B **10** L527
[34] Ho Y K 1981 *Phys. Rev.* A **23** 2137
[35] Ho Y K 1984 *J. Phys.* B **17** L695
[36] Chung K T and Davis B F 1982 *Phys. Rev.* A **26** 3278
[37] Bentley M 1990 *Phys. Rev.* A **42** 3826
[38] Salomonson S, Carter S L and Kelly H P 1989 *Phys. Rev.* A **39** 5111
[39] Moccia R and Spizzo P 1987 *J. Phys.* B **20** 1423
[40] Tang J Z, Watanabe S and Matsuzawa M 1993 *Phys. Rev.* A **48** 841
[41] Zou Y, Fang Q Y and Li J M 1998 *Chin. Phys. Lett.* **15** 175
[42] Gorczyca T W, Rubensson J E, Såthe C, Ström M, Agåker M, Ding D J, Stranges S, Richter R and Alagia M 2000 *Phys. Rev. Lett.* **85** 1202
[43] Grant I P, Mckenzie B J, Norrington P H, Mayers D F and Pyper N C 1980 *Comput. Phys. Commun.* **21** 207
[44] Dyall K G, Grant I P, Johnson C T, Parpia F A and Plummer E P 1989 *Comput. Phys. Commun.* **55** 425
[45] Fritzsche S, Fischer C F and Dong C Z 2000 *Comput. Phys. Commun.* **124** 340
[46] Fritzsche S, Aksela H, Dong C Z, Heinäsmäki S and Sienkiewicz J E 2003 *Nucl. Instr. Meth. Phys. Res.* B **205** 93
[47] Fritzsche S 2001 *Journal of Electron Spectroscopy and Related Phenomena* **114–116** 1155
[48] Wan J J, Dong C Z, Sang C C, Ding X B, Xie L Y and Jiang J 2007 *Journal of Physics:Conference Series* **58** 367
[49] Sang C C, Wan J J, Dong C Z, Ding X B and Jiang J 2008 *Acta Phys. Sin.* **57** 2152 (in Chinese)
[50] Roos B O, Taylor P R and Siegbahn P E M 1980 *Chem. Phys.* **48** 157
[51] Parpia F A, Fischer C F and Grant I P 1996 *Comput. Phys. Commun.* **94** 249
[52] Frankowski K and Pekeris C L 1966 *Phys. Rev.* A **146** 46
[53] Freund D E, Huxtable B D and Morgan III J D 1984 *Phys. Rev.* A **29** 980
[54] Parpia F A and Grant I P 1990 *J. Phys.* B **23** 211
[55] Wang G L private discussion
[56] Duan Y S, Liu Y X and Zhang L J 2004 *Chin. Phys. Lett.* **21** 1714
[57] Norrington P H and Grant I P 1987 *J. Phys.* B **20** 4869